

New visualizations for Monte Carlo simulations

Nathan Robertson

Department of Statistics

University of California, Riverside

nathan.robertson@email.ucr.edu

James M. Flegal

Department of Statistics

University of California, Riverside

jflegal@ucr.edu

Galin L. Jones

School of Statistics

University of Minnesota

galin@umn.edu

Dootika Vats

Department of Statistics

University of Warwick

dootika.vats@gmail.com

March 23, 2022

Abstract

In Monte Carlo simulations, samples are obtained from a target distribution in order to estimate various features. We present a flexible class of visualizations for assessing the quality of estimation, which are principled, practical, and easy to implement. To this end, we establish joint asymptotic normality for any collection of means and quantiles. Using the limit distribution, we construct $1 - \alpha$ level simultaneous confidence intervals, which we integrate within visualization plots. We demonstrate the utility of our visualizations in various Monte Carlo simulation settings including Monte Carlo estimation of expectations and quantiles, Monte Carlo simulation studies, and Bayesian analyses using Markov chain Monte Carlo sampling. The marginal-friendly interpretation enables practitioners to visualize simultaneous uncertainty, a substantial improvement from current visualizations.

Keywords. Asymptotic normality, Monte Carlo, Markov chain Monte Carlo, quantile limit theorems, simulation studies, strongly mixing, visualizations.

1 Introduction

The analysis of output obtained from a Monte Carlo simulation is an essential part of ensuring reliable simulation studies. We propose new visualization tools based on simultaneous confidence intervals with a desired confidence level, which are narrower than conservative approaches (e.g. Bonferonni). Our focus is on Monte Carlo settings including sampling

independent and identically distributed (IID) random variables and correlated sampling of random variables arising from strongly mixing sequences or Markov chain Monte Carlo (MCMC). However, the conditions we require allows our approach to be used more broadly.

Suppose Monte Carlo samples are used to estimate features of a distribution, say π , by generating (possibly correlated) samples from π . This scenario frequently arises in physical and mathematical problems when other approaches are intractable. Typically, the interest is in estimating several parameters simultaneously, which may include both expectations and quantiles. Further, there is often dependence between the parameters. For example, simulation studies often compare statistical techniques or models using IID replications to estimate multiple quantities simultaneously (e.g. estimation error and prediction error). Alternatively, a Bayesian may be interested in estimating multiple posterior means along with credible intervals simultaneously.

Due to variability in repeated simulations, it is imperative to include estimated simulation uncertainty with feature estimates to give a sense of the simulation’s quality and reliability. Reporting simulation uncertainty usually amounts to reporting Monte Carlo standard errors or confidence intervals. We note reporting only the Monte Carlo sample size (or effective sample size) does not, in general, provide the necessary indication of simulation uncertainty; see Flegal et al. (2008) and Koehler et al. (2009) for additional discussion.

When standard errors are reported, they are almost always univariate, ignoring multiplicity and dependence among parameters. One can address this by providing multivariate confidence regions when estimating expectations (Vats et al., 2018; Vats et al., 2019), but this does not address the estimation of quantiles or the simultaneous estimation of means and quantiles. More importantly, visualization and interpretation of confidence regions is problematic for multi-dimensional quantities. Most current visualizations ignore Monte Carlo uncertainty altogether and report quantities from empirical marginal distributions, e.g., by using sample boxplots. Software such as **Stan** (Stan Development Team, 2018) and **tidybayes** (Kay, 2018) suffer from the same drawbacks when reporting credible intervals or prediction intervals. We provide a flexible and novel class of visualizations for assessing the quality of simultaneous estimation of means and quantiles from Monte Carlo simulations.

Consider a motivating example estimating the mean and $(.10, .90)$ -quantiles for a three component mixture of normal densities. We simulate draws using a Metropolis-Hastings (MH) random walk to estimate the 3-dimensional quantity of interest and its corresponding 3×3 asymptotic covariance matrix. Figure 1 shows 90% simultaneous confidence intervals superimposed on a plot containing an empirical density estimate. Figure 1 indicates substantial uncertainty around the estimates when only 1,000 samples are drawn and that

50,000 samples provide far more certainty. A closer examination reveals that the confidence regions displayed around each quantity of interest have different lengths.

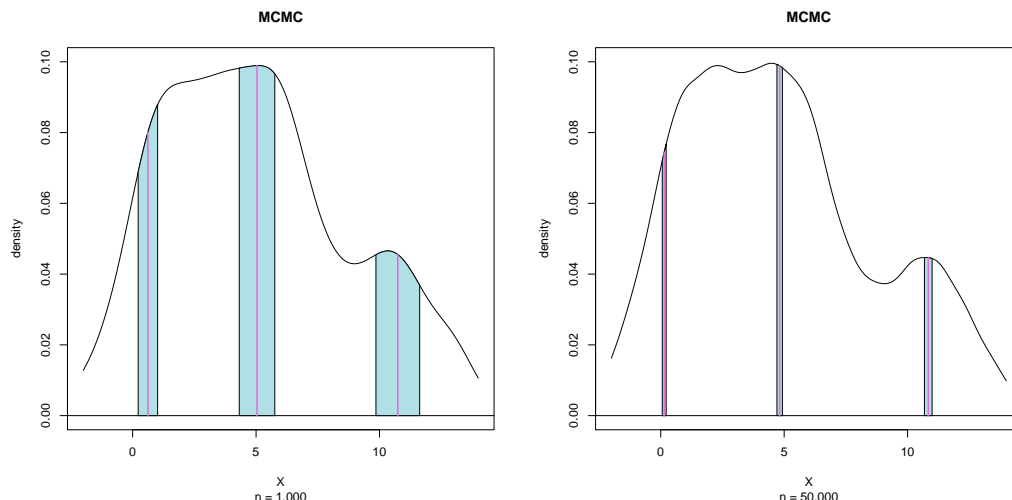


Figure 1: Visualization of simultaneous uncertainty bounds for the mean and (.10,.90)-quantiles.

Figure 1 enables practitioners to visualize simultaneous simulation uncertainty. It clearly illustrates both the variability of the distribution, π , and the uncertainty in estimation from a using Monte Carlo simulation without overemphasizing point estimates and hence follows suggested practice (see e.g. Shubin, 2015). Our visualization tools apply much more broadly than the motivating example in Figure 1. For example, one can consider more than one parameter, additional means and quantiles, or even boxplots. We illustrate these in a series of examples, but many other uses of our methodology are possible.

The techniques proposed here provide simultaneous intervals for any combination of quantiles and expectations. That is, the parameters of interest will be in their respective confidence intervals simultaneously with the desired level of significance, say $1 - \alpha$. It is important to note that our results are neither pointwise intervals each having coverage probability $1 - \alpha$ nor conservative simultaneous intervals (e.g. Bonferonni) where the overall coverage probability often greatly exceeds $1 - \alpha$.

To construct simultaneous confidence intervals with the desired level of significance, we propose a parametric approach that utilizes joint asymptotic normality for the Monte Carlo error of expectations and quantiles. To this end, our first result establishes asymptotic normality of sample means and quantiles where we also provide estimators for the covariance matrix of the asymptotic normal distribution. Our result holds for settings where a

strong law, a central limit theorem (CLT) for sample means, and a Bahadur (1966) quantile representation hold. We illustrate sufficient conditions for IID sampling, strongly mixing processes, and Markov chain sampling. Therefore, techniques described here are widely applicable.

Given joint asymptotic normality, one could construct marginal confidence intervals, conservative simultaneous intervals, or confidence regions with $1 - \alpha$ coverage based on an ellipsoid. However, each of these suffer from drawbacks mentioned previously. Instead, we construct simultaneous intervals using joint asymptotic normality to obtain a $1 - \alpha$ confidence hyper-rectangle. As we illustrate later, our algorithm reduces to a univariate optimization problem. These simultaneous intervals form the building blocks for the proposed visualization techniques.

We implement our methodology and visualizations in three examples. Our first example continues the three component mixture of normals. Since the truth is known in this example, we assess finite sample performance of simultaneous confidence intervals by comparing coverage probabilities with other univariate and multivariate methods. This Monte Carlo simulation study illustrates the utility of our visualization tools. Our second example considers another Monte Carlo simulation study comparing estimation error for different regression methods, where we equip the standard side-by-side boxplots with simultaneous confidence intervals. The resulting plot is especially useful in indicating whether sufficient Monte Carlo replications have been run. Our third example illustrates a couple of different marginal-friendly visualizations for Bayesian inference on two sets of features from a posterior distribution.

The remainder is organized as follows. In Section 2, we present the joint asymptotic distribution of sample means and quantiles for both independent and dependent sequences. Section 3 presents a univariate optimization method for obtaining simultaneous confidence intervals. Section 4 presents example visualizations for the three component mixture of normals, two Monte Carlo simulations studies, and a Bayesian analysis. We conclude with a discussion in Section 5.

2 Joint asymptotic distribution

Consider a probability distribution, π , with support $\mathbf{X} \subseteq \mathbb{R}^d, d \geq 1$. We develop a joint asymptotic distribution for the estimators of p_1 expectations and p_2 quantiles associated with π using a process $X = \{X_1, X_2, \dots\}$. We will be more specific below about what must be assumed about X .

First, suppose $g : \mathsf{X} \rightarrow \mathbb{R}^{p_1}$ and consider estimating p_1 expectations

$$\theta_g = E_\pi [g(X)] = \int_{\mathsf{X}} g(x) \pi(dx) .$$

We assume that with probability one, as $n \rightarrow \infty$,

$$\bar{g}_n = \frac{1}{n} \sum_{j=1}^n g(X_j) \rightarrow \theta_g \quad (1)$$

and that the sampling distribution for the Monte Carlo error, $\bar{g}_n - \theta_g$, can be obtained via a CLT. That is, there exists a $p_1 \times p_1$ positive definite matrix Σ_g such that, as $n \rightarrow \infty$,

$$\sqrt{n}(\bar{g}_n - \theta_g) \xrightarrow{d} N_p(0, \Sigma_g) . \quad (2)$$

The formulation and estimation of Σ_g will be discussed in detail later.

Now consider estimating p_2 quantiles associated with π . These quantiles could be with respect to any functional of X and not merely the components of X or $g(X)$. Unfortunately, this level of generality leads to somewhat cumbersome notation. Define a function $h : \mathsf{X} \rightarrow \mathbb{R}^{p_2}$ such that $h(X) = (h_1(X), \dots, h_{p_2}(X))'$ where each $h_i(X)$ represents some functional of interest. Further, define $Q = (q_1, \dots, q_{p_2})'$ where q_i is the desired quantile from $h_i(X)$. We note that two functionals $h_i(X)$ and $h_j(X)$ may be the same, as it is often the case that multiple quantiles of the same functional are being estimated. For $V = h(X)$, the p_2 quantiles of interest are associated with marginal distribution functions of V , say $F_{h_i}(v)$, which we assume are absolutely continuous with continuous densities $f_{h_i}(v)$. Finally, define the q_i -quantile associated with F_{h_i} as

$$\xi_{q_i} = F_{h_i}^{-1}(q_i) = \inf\{v : F_{h_i}(v) \geq q_i\},$$

where our interest is in estimating the vector of p_2 quantiles denoted

$$\phi = (\xi_{q_1}, \dots, \xi_{q_{p_2}})' .$$

Estimation is straightforward using marginal order statistics from $h(X)$. That is, let $\hat{\xi}_{q_i} = h_i(X)_{[nq_i]:n}$ be the $[nq_i]^{th}$ order statistic of $h_i(X)$ and denote the vector of p_2 estimated quantiles as

$$\hat{\phi}_n = (\hat{\xi}_{q_1}, \dots, \hat{\xi}_{q_{p_2}})' .$$

A strong law for estimators of $F_{h_i}(v)$ is enough to ensure $\hat{\phi}_n \rightarrow \phi$ as $n \rightarrow \infty$ with probability one (see e.g. Doss et al., 2014; Serfling, 1981).

The joint asymptotic distribution for p_1 expectations and p_2 quantiles can be established using the Bahadur quantile representation. To this end, define empirical distributions for F_{h_i} as

$$\bar{F}_{h_i}(v) = \frac{1}{n} \sum_{j=1}^n I(h_i(X_j) \leq v),$$

with vectorized representation

$$\bar{F}_h(v) = \left(\bar{F}_{h_1}(v_1), \dots, \bar{F}_{h_{p_2}}(v_{p_2}) \right)'.$$

Since probabilities can be expressed as expectations of indicator functions, the strong law ensures that, as $n \rightarrow \infty$, $\bar{F}_h(\phi) \rightarrow Q$ with probability one. Further, the CLT at (2) can be re-expressed as

$$\sqrt{n} \left(\begin{pmatrix} \bar{g}_n \\ 1 - \bar{F}_h(\phi) \end{pmatrix} - \begin{pmatrix} \theta_g \\ 1 - Q \end{pmatrix} \right) \xrightarrow{d} N_{p_1+p_2} \left(0, \Sigma = \begin{pmatrix} \Sigma_g & \Sigma_{gh} \\ \Sigma_{hg} & \Sigma_h \end{pmatrix} \right) \quad (3)$$

as $n \rightarrow \infty$, where Σ and Σ_h are positive definite covariance matrices, and $\Sigma_{gh} = \Sigma'_{hg}$ are the $p_1 \times p_2$ cross-covariance matrices. Next, consider the Bahadur (1966) quantile representation

$$\hat{\xi}_{q_i} = \xi_{q_i} + \frac{(1 - \bar{F}_{h_i}(\xi_{q_i})) - (1 - q_i)}{f_{h_i}(\xi_{q_i})} + r_{n,q_i}, \quad (4)$$

where r_{n,q_i} is $o_p(n^{-1/2})$. Then the joint distribution for estimation of p_1 expectations and p_2 quantiles is established in the following theorem.

Theorem 1. *Suppose a strong law, CLT, and Bahadur quantile representation hold as at (1), (3), and (4), respectively. Let A_h be a $p_2 \times p_2$ diagonal matrix with i^{th} diagonal elements $f_{h_i}(\xi_{q_i})$. If*

$$\Lambda = \begin{pmatrix} I_{p_1} & 0_{p_1 \times p_2} \\ 0_{p_2 \times p_1} & A_h \end{pmatrix},$$

then, as $n \rightarrow \infty$,

$$\sqrt{n} \begin{pmatrix} \bar{g}_n - \theta_g \\ \hat{\phi}_n - \phi \end{pmatrix} \xrightarrow{d} N(0, \Lambda^{-1} \Sigma \Lambda^{-1}). \quad (5)$$

Proof. Let $R_n = (r_{n,q_1}, \dots, r_{n,q_{p_2}})'$, then by (4),

$$(1 - \bar{F}_h(\phi)) - (1 - Q) = A_h (\hat{\phi}_n - \phi) + A_h R_n \xrightarrow{P} A_h (\hat{\phi}_n - \phi). \quad (6)$$

Combining (3) and (6) we have

$$\begin{aligned}\sqrt{n} \left(\begin{pmatrix} \bar{g}_n \\ 1 - \bar{F}_h(\phi) \end{pmatrix} - \begin{pmatrix} \theta_g \\ 1 - Q \end{pmatrix} \right) &= \sqrt{n} \begin{pmatrix} \bar{g}_n - \theta_g \\ A_h(\hat{\phi}_n - \phi) \end{pmatrix} + o_p(1) \\ &= \sqrt{n} \Lambda \begin{pmatrix} \bar{g}_n - \theta_g \\ \hat{\phi}_n - \phi \end{pmatrix} + o_p(1).\end{aligned}$$

□

Using Theorem 1 requires estimation of Λ^{-1} and Σ . Since Λ is a diagonal matrix with non-zero diagonals, its inverse Λ^{-1} is readily available. Then kernel density estimators with a Gaussian kernel can be used to estimate $f_{h_i}(\hat{\xi}_{q_i})$, and hence estimate Λ . The matrix Σ requires more specific attention since IID and dependent sampling schemes yield different structures of Σ . We discuss these differences in the next two sections, both of which are implemented in R as part of the supplementary material.

2.1 Independent sequences

Suppose $X = \{X_1, X_2, \dots\}$ are IID realizations from π . The strong law and CLT hold for estimating θ_g provided, $E_\pi \|g\| < \infty$ and $E_\pi \|g\|^2 < \infty$, respectively. Since $|\bar{F}_h(\cdot)| \leq 1$, these conditions also ensure the joint distribution at (3). The Bahadur quantile representation at (6) requires $0 < f_{h_i}(\xi_{q_i}) < \infty$ and continuity of f_{h_i} in a neighborhood of ξ_{q_i} for all i (Ghosh, 1971). This is weaker than our prior assumption that $F_{h_i}(v)$ is absolutely continuous with continuous density $f_{h_i}(v)$, which is required for more general processes.

Joint asymptotic distributions for IID sampling have received substantial attention. Laplace found the joint asymptotic distribution of the sample mean and the sample median (Stigler, 1973). Ferguson (1998) provides a nice derivation for a sample mean and an arbitrary quantile along with an expression of the covariance (also see Lin et al., 1980). This result can be generalized to sample means and arbitrary quantiles associated with distinct marginal random variables. Babu and Rao (1988) provide an expression of the covariance between two quantiles. These results yield an exact, albeit complicated, expression for $\Lambda^{-1}\Sigma\Lambda^{-1}$ from (5). Suppose $Y_j = \left(g(X_j), I(h(X_j) > \hat{\phi}_n)\right)'$, then our R implementation estimates Σ by the sample covariance of $\{Y_1, Y_2, \dots, Y_n\}$.

2.2 Dependent sequences

This section provides conditions for the strong law, CLT, and Bahadur quantile representation when $X = \{X_1, X_2, \dots\}$ is a dependent sequence. Specifically, we consider a stationary

strongly mixing (or α -mixing) setting and its connection to MCMC simulations. The discussion here is not exhaustive and does not provide minimal known conditions; see Bradley (1986, 2005) and Jones (2004) for more information.

The strong law holds for estimating θ_g , provided $E_\pi \|g\| < \infty$ and X is strongly mixing (Blum and Hanson, 1960). Since Harris ergodic Markov chains are strongly mixing, the strong law holds under the same moment conditions (Jones, 2004; Meyn and Tweedie, 2009). Ibragimov (1962) provides a CLT if there exists a $\delta > 0$ such that $E_\pi \|g\|^{2+\delta} < \infty$ and X mixes sufficiently fast. Corollary 2 of Jones (2004) (using additional results from Ibragimov and Linnik, 1971) provides a CLT for geometrically and polynomial ergodic Markov chains. Yoshihara (1995) provides the Bahadur quantile representation at (6) when $F_{h_i}(v)$ is absolutely continuous with continuous density $f_{h_i}(v)$ such that $0 < f_{h_i}(\xi_{q_i}) < \infty$ and X mixes sufficiently fast. Such a mixing condition holds for polynomial ergodic Markov chains (Jones, 2004). Wang et al. (2011) weakens these mixing conditions, but their Bahadur quantile representation is not applicable for MH algorithms.

Recall that $Y_j = \left(g(X_j), I(h(X_j) > \hat{\phi})\right)'$. For a stationary strongly mixing sequence, an expression for Σ is

$$\Sigma = \text{Cov}(Y_j, Y_j) + \sum_{i=1}^{\infty} [\text{Cov}(Y_j, Y_{j+i}) + \text{Cov}(Y_j, Y_{j-i})]'. \quad (7)$$

Estimation of Σ at (7) is a well studied problem and may be accomplished using batch means (Chen and Seila, 1987; Vats et al., 2019), weighted batch means (Liu and Flegal, 2018), spectral variance (Andrews, 1991; Priestley, 1981; Vats et al., 2018), initial sequence (Dai and Jones, 2017), recursive (Chan and Yau, 2017) or regenerative sampling estimators (Hobert et al., 2002; Seila, 1982).

Due to computational simplicity we restrict our attention to batch means estimators with batch size equal to $\lfloor \sqrt{n} \rfloor$. Let $n = ab$ where a is the number of batches and b is the batch size. The mean for the k^{th} batch is $\bar{Y}_k(b) = b^{-1} \sum_{t=1}^b Y_{kb+t}$ and the overall mean is $\bar{Y} = a^{-1} \sum_{k=1}^a \bar{Y}_k(b)$. Then the batch means estimator with batch size b is

$$\hat{\Sigma} = \frac{b}{a-1} \sum_{k=0}^{a-1} (\bar{Y}_k(b) - \bar{Y})(\bar{Y}_k(b) - \bar{Y})'.$$

3 Simultaneous confidence intervals

We now develop simultaneous confidence intervals for the p -dimensional vector $(\theta_g, \phi)'$ having a $1 - \alpha$ coverage level. The general procedure will use lower and upper bounds on the

confidence region and search over possible values between.

Confidence regions in multivariate settings often take one of two approaches, a region of minimum volume or intervals based on marginal distributions. A minimum volume region takes an elliptical form for a limiting multivariate normal distribution. The location of this ellipsoid is determined by the mean vector while the shape is determined by the eigenvalues and eigenvectors of the covariance matrix. Unfortunately, visualizing an ellipsoid is challenging when $p \geq 4$, hence they are rarely presented in Monte Carlo output analysis. It is more common to report confidence intervals based on the marginal distributions creating a hyper-rectangular confidence region. The location of the hyper-rectangle is determined by the mean vector while the diagonals of the covariance matrix, i.e. the marginal variances, determine the length of each side. The popularity of hyper-rectangles stems from the fact they can be easily reported and visualized. We improve hyper-rectangular confidence regions by incorporating the full covariance information to determine appropriate marginal confidence levels yielding a simultaneous confidence level of $1 - \alpha$.

First, consider a hyper-rectangular confidence region based on marginal intervals each with confidence level $1 - \alpha$, i.e. intervals not adjusted for multiplicity. Denote such a region as C_{LB} . If the random variables, $(\bar{g}_n, \hat{\phi}_n)$, are perfectly correlated, this will yield the correct overall coverage level while yielding undercoverage in any other case. The region C_{LB} will act as the lower bound for our coverage level. We consider Bonferroni corrected simultaneous intervals as an upper bound, denoted C_{UB} . If all components of $(\bar{g}_n, \hat{\phi}_n)$ are uncorrelated, C_{UB} yields the approximately correct overall coverage level. However, overcoverage occurs in any other case. Assuming a fixed estimate of $\Lambda^{-1}\Sigma\Lambda^{-1}$, intervals of these forms maintain a constant aspect ratio in the axes. That is, the ratio of the lengths of the intervals in C_{LB} and C_{UB} is the same for all components. This property allows searching for a hyper-rectangular confidence region between C_{LB} and C_{UB} with the correct confidence level $1 - \alpha$ to reduce to a one-dimensional line search. A sketch of two-dimensional confidence regions and the appropriate line search is pictured in Figure 2.

Consider a hyper-rectangular confidence region $\mathcal{C}_{SI}(z)$ with critical value z constructed using estimators of $\Lambda^{-1}\Sigma\Lambda^{-1}$ described in Section 2. We are interested in $P(X \in \mathcal{C}_{SI}(z))$ where X is approximately from a multivariate normal distribution with covariance matrix $\hat{\Lambda}^{-1}\hat{\Sigma}\hat{\Lambda}^{-1}$. For $C_{LB} = \mathcal{C}_{SI}(z_{1-\alpha/2})$, we have $P(X \in C_{LB}) \leq (1 - \alpha)$ and for $C_{UB} = \mathcal{C}_{SI}(z_{1-\alpha/2p})$, we have $P(X \in C_{UB}) \geq (1 - \alpha)$. Since $P(X \in \mathcal{C}_{SI}(z))$ is strictly increasing as z increases, we can use the bisection method between $z_{1-\alpha/2}$ and $z_{1-\alpha/2p}$ to find z^* such that $P(X \in \mathcal{C}_{SI}(z^*)) \approx (1 - \alpha)$.

The solution using the bisection method will be up to some error tolerance $\epsilon = P(X \in \mathcal{C}_{SI}(z^*)) - (1 - \alpha)$. The choice of ϵ deserves some care depending on how $P(X \in \mathcal{C}_{SI}(z))$ is

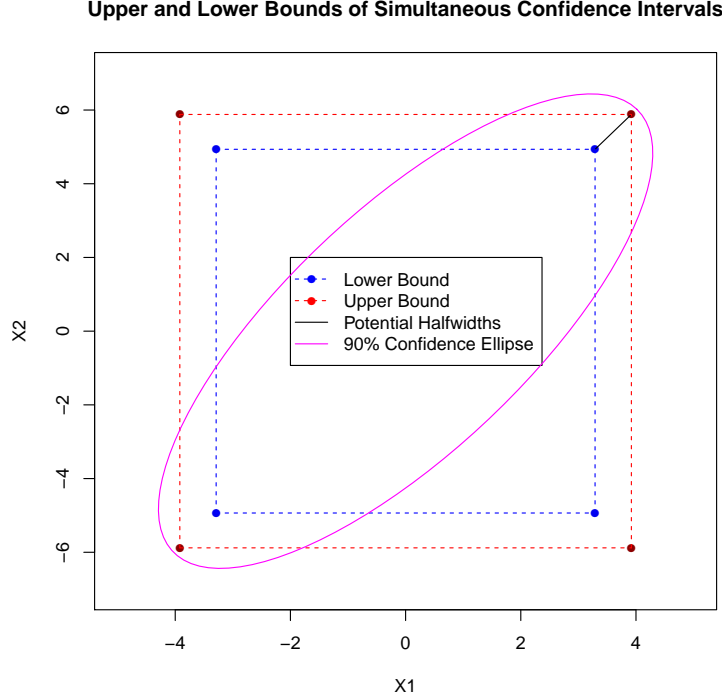


Figure 2: Plot of C_{LB} (blue) and C_{UB} (red) from a 90% confidence region for a bivariate normal distribution with component variances 4 and 9. The black line in the first quadrant indicates the potential search values to achieve the desired overall coverage level.

calculated. We rely on the function `pmvnorm` from the R package `mvtnorm` (Genz et al., 2018) which provides an error bound on the probability calculated. We conducted several simulations varying covariance, dimension, and probability values. The largest error recorded was approximately .002 with most errors less than .001. Results from this study are available upon request. We recommend setting $\epsilon = .001$ or $\epsilon = .002$.

4 Example visualizations

This section demonstrates the flexibility of our class of visualizations in various Monte Carlo simulation settings. In each example, we identify a combination of means and quantiles of interest, obtain $1 - \alpha$ level simultaneous confidence intervals, and integrate the intervals within a standard plot. The full R code is available as part of the supplementary material to ensure reproducibility of simulations and plots presented below.

4.1 Mixture of normal distributions

This section provides details for the mixture of normal distributions example from the introduction. In the subsequent section we will demonstrate the accuracy of our procedure by estimating coverage probabilities via a Monte Carlo simulation. Let X be a random variable distributed according to a mixture of 3 normal distributions, with density

$$f_X(x) = .3f_1(x; 1, 2.5) + .5f_2(x; 5, 4) + .2f_3(x; 11, 3). \quad (8)$$

where $f_j(x; \mu_j, \sigma_j^2)$ is the density of the j^{th} mixture component with mean μ_j and variance σ_j^2 . We consider simultaneous estimation of the mean, .10 quantile, and .90 quantile denoted μ , $\xi_{.10}$, and $\xi_{.90}$, respectively. Specifically, we have $(\theta_g, \phi)' = (\mu, \xi_{.10}, \xi_{.90})$ from (5). If f_X is a posterior density, then $(\xi_{.10}, \xi_{.90})$ would be characterized as an 80% credible interval.

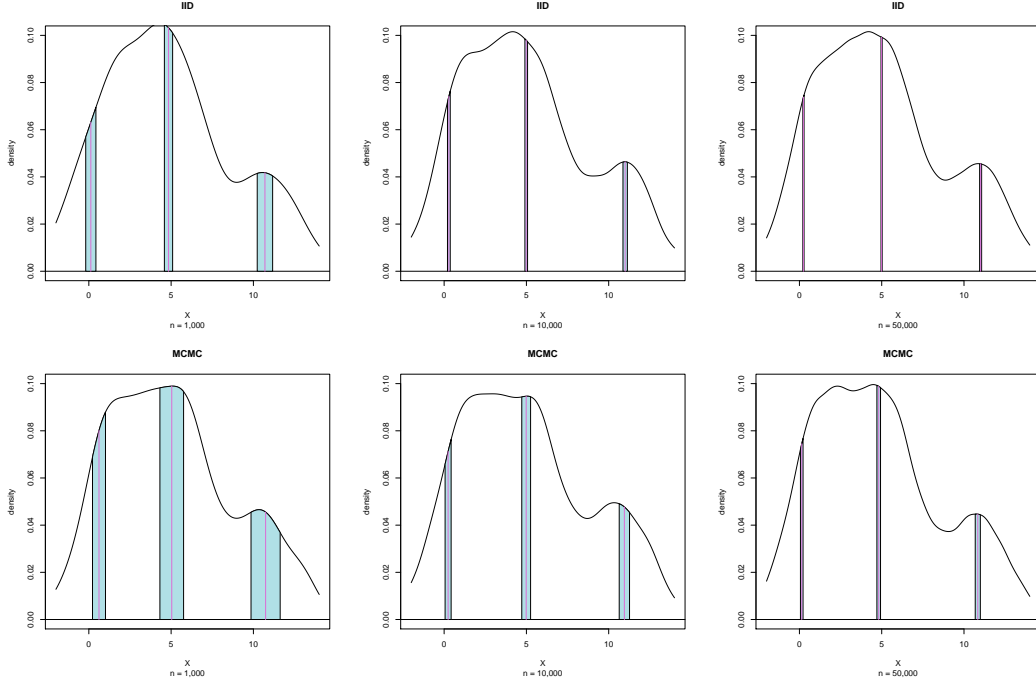


Figure 3: Simultaneous 90% confidence intervals of the mean, .10 quantile, and .90 quantile from a mixture of normal distributions.

We collect IID samples from (8) and estimate $(\theta_g, \phi)'$ and $\Lambda^{-1}\Sigma\Lambda^{-1}$ as described in Section 2. We then calculate $C_{SI}(z^*)$ at the 90% confidence level and estimate the density to create our visualization in the top row of Figure 3. The estimates of $(\theta_g, \phi)'$ are represented by purple lines with the blue region around each estimate representing the simultaneous simulation uncertainty. As the number of samples increases, simulation uncertainty decreases.

Another point of interest is in the different amount of simulation uncertainty surrounding $\xi_{.10}$ and $\xi_{.90}$. The shape of the density is asymmetric, thus the two quantiles occur at different density values. This affects the value of Λ^{-1} and contributes to the different lengths of the error regions around each estimate.

To illustrate our methods for a dependent sampling case we use a random walk MH sampler with proposal distribution $N(0, 9)$. We estimate $(\theta_g, \phi)'$ and $\Lambda^{-1}\Sigma\Lambda^{-1}$ as described in Section 2. Simultaneous confidence intervals are presented in the bottom row of Figure 3 where the MCMC plots contain notably more simulation uncertainty than the IID case. This occurs due to within chain correlation captured by the infinite sum at (7). One measure of this is effective sample size (ESS), which estimates how many IID samples a correlated sample is equivalent to. Our MH sampler had an ESS (Vats et al., 2019) to n ratio of about .2, hence it is unsurprising the IID $n = 10,000$ and MCMC $n = 50,000$ plots in Figure 3 illustrate similar levels of simulation uncertainty.

4.2 Coverage probabilities

This section continues the mixture normal distributions where we illustrate two points. First, we demonstrate simultaneous confidence intervals $\mathcal{C}_{SI}(z^*)$ have the correct coverage probability in finite samples via a Monte Carlo simulation. Second, we illustrate the utility of our visualization tools for this Monte Carlo simulation.

To examine the coverage properties of our estimating procedure, n IID samples are again collected from (8) to estimate $(\theta_g, \phi)'$. Using the same simulated data, simultaneous confidence intervals $\mathcal{C}_{SI}(z^*)$, uncorrected marginal intervals C_{LB} , and simultaneous Bonferroni intervals C_{UB} are calculated at the 80% and 90% confidence levels for which we record whether each region contains the true value. The true value of $\theta_g = \mu$ is expressible as the sum of each mixture mean multiplied by the mixture probability yielding $\mu = 5$. To calculate $\phi = (\xi_{.10}, \xi_{.90})$, a numerical optimization technique may be used to integrate $\int_{-\infty}^y f_X(x)dx$ over values of y until the desired probability is found. We use the integrate function in R and found $\xi_{.10} = .2544116$ and $\xi_{.90} = 11.0143117$ with absolute error less than $2.5e-6$. Thus, we have six binary outcomes, one for each region and confidence level combination, which are naturally correlated since we are using the same simulated data. We replicate this sampling scheme 2,000 times to create a Monte Carlo sample of six Bernoulli estimates based on the n samples. We then calculate simultaneous intervals, using Theorem 1, with overall 95% confidence level and plot the results in the top row of Figure 4. This procedure was repeated for $n = 500, 1000, 5000$, and 10000 .

Within each plotting window, Figure 4 shows observed coverage probabilities for the uncorrected marginal intervals C_{LB} , simultaneous confidence intervals $\mathcal{C}_{SI}(z^*)$, and simul-

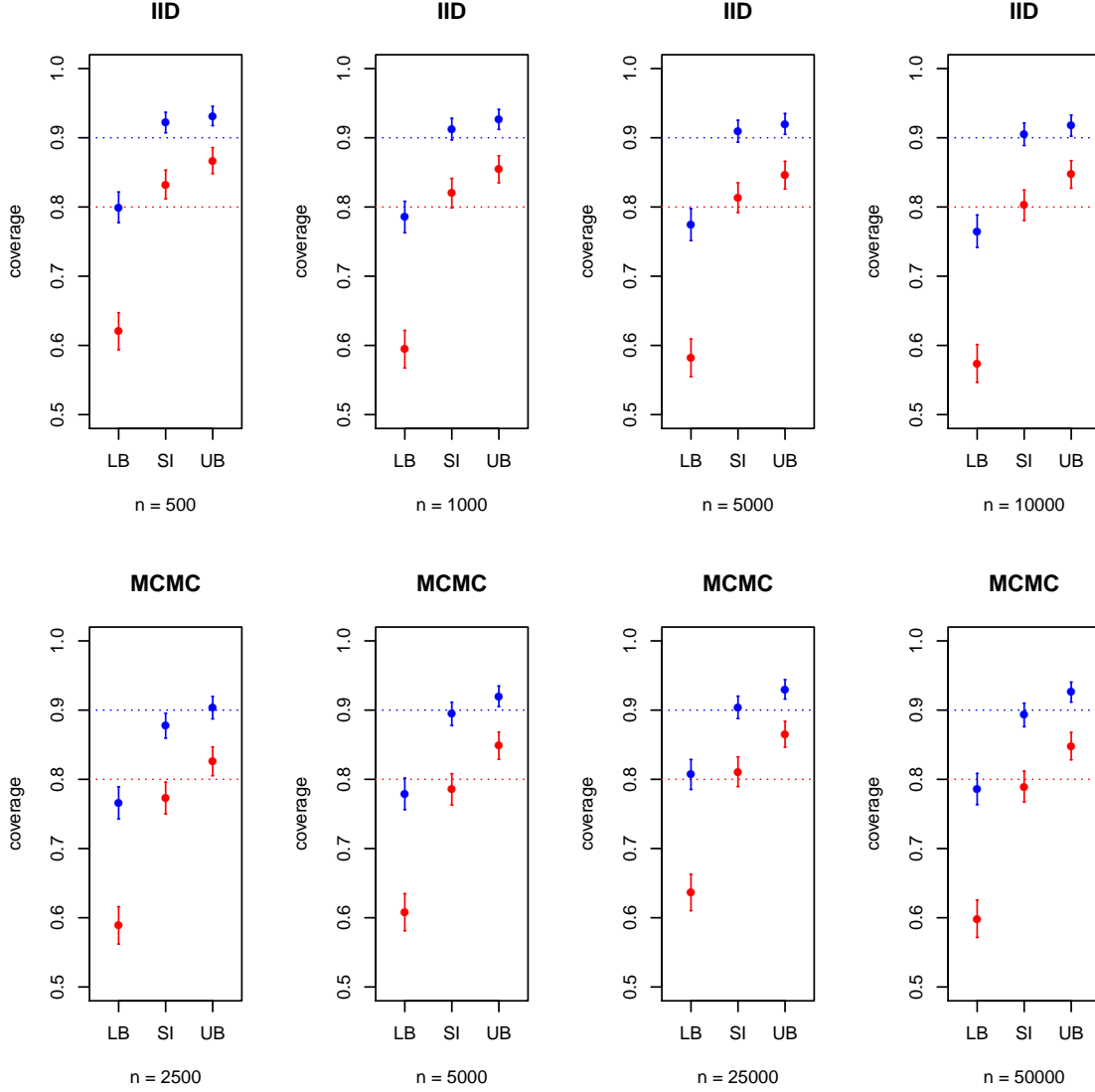


Figure 4: Simultaneous 95% confidence intervals for coverage probabilities based on 2,000 replications comparing uncorrected marginal intervals C_{LB} , simultaneous confidence intervals $C_{SI}(z^*)$, and simultaneous Bonferonni intervals C_{UB} .

taneous Bonferonni intervals C_{UB} from left to right. The color of each confidence interval indicates the nominal level with the target denoted by a dashed line of the same color. Clearly, C_{LB} yields significant undercoverage while failing to ever capture the nominal coverage probability within any of its interval estimates. For $C_{SI}(z^*)$, the confidence intervals contain the nominal level as the sample size increases illustrating simultaneous intervals yield coverage close to the nominal level. Bonferonni intervals, C_{UB} , approach a value

which overestimates the nominal level. This overcoverage is relatively small since the adjustment is based on a small number of quantities. However, estimation procedures of higher dimensionality will correspond to more conservative estimates for the upper bound. Usually in a Monte Carlo simulation such as this, only point estimates would be provided in a table. Then the difference between simultaneous and Bonferonni intervals would be difficult to observe and virtually impossible to argue its significance.

Now consider the dependent sampling case using our random walk MH sampler with proposal distribution $N(0, 9)$. All simulation settings remain the same except sample size which we take to be five times larger based on our previous discussion on ESS. That is, we consider $n = 2500, 5000, 25000$, and 50000 . The bottom row of Figure 4 provides results from the MCMC simulation, which are consistent with the IID results.

4.3 Side-by-side boxplots

Performance of statistical methodologies is often illustrated by loss function comparisons with existing methods over repeated simulations. Visualization of such Monte Carlo studies is often done using side-by-side boxplots. Our visualization tools can be used to illustrate the variability in the estimation of the quantiles in the boxplots. More importantly, the visualization provides a tool to assess whether sufficient replications have been used.

Consider a comparison of lasso (Tibshirani, 1996), ridge (Hoerl and Kennard, 1970), and ordinary least squares (OLS) regressions. Let $y \in \mathbb{R}^{100}$ be the observed response vector, X be a 100×21 dimensional matrix of covariates, and $\beta^* \in \mathbb{R}^{21}$ be the true regression coefficient vector. For $\epsilon \sim N_{100}(0, I_{100})$, our data generating model is

$$y = X\beta^* + \epsilon.$$

We set β^* to be such that the first 11 elements are zero, and the last 10 are random draws from a normal distribution with mean 0 and variance 2. The matrix X is constructed such that the first column is all 1s, and the rows of X_{-1} , the matrix X with the first column removed, are drawn from $N_{20}(0, \Omega)$, where the ij th entry of Ω is $.90^{|i-j|}$. Over repeated simulations, we fit a lasso, ridge, and OLS regressions to estimate the vector of coefficients. Lasso and ridge estimates are obtained using the `glmnet` package (Friedman et al., 2009) with tuning parameters chosen using cross-validation. In each replication, we note the squared estimation error of the estimated coefficient, $\hat{\beta}$, that is, $\|\hat{\beta} - \beta^*\|^2$. We repeat the simulation for 100, 500, and 2000 Monte Carlo replications. Figure 5 presents the resulting boxplots with and without simultaneous confidence intervals.

Recall a box in the boxplot has 25%, 50%, and 75% quantiles. To make our red and

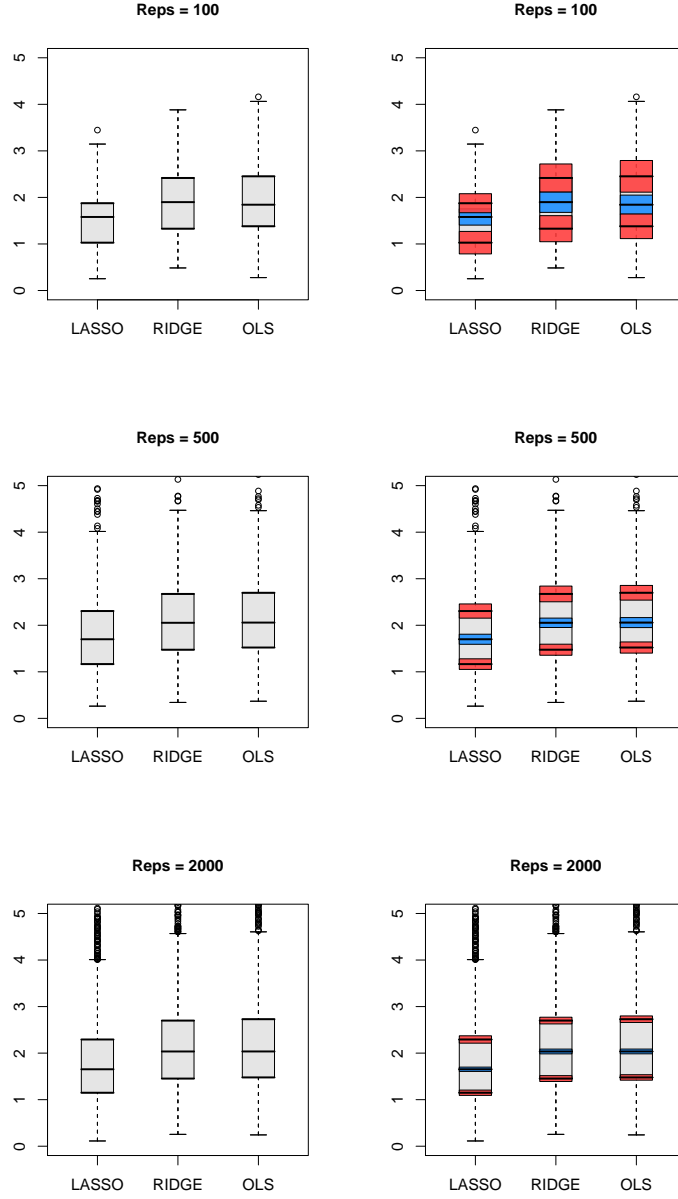


Figure 5: Boxplots of squared estimation error for lasso, ridge, and OLS with and without simultaneous confidence intervals. Monte Carlo sample size increases top to bottom.

blue confidence intervals, we appeal to the 9-dimensional joint asymptotic distribution for IID sequences for these quantiles, along with the line search algorithm of Section 3. The simultaneous confidence intervals immediately indicate that with only 100 Monte Carlo replications, all quantile estimates have large variation. This variability is significantly

improved with 2000 Monte Carlo replications. Such an analysis is impossible with the plots on the left.

4.4 Visualizations for Bayesian analysis

Our final example integrates simultaneous confidence intervals within standard density plots and boxplots for Bayesian analysis. The specific example we consider is a Gibbs sampler targeting the posterior distribution for a hierarchical normal model, analyzing the school data of Gelman et al. (2004).

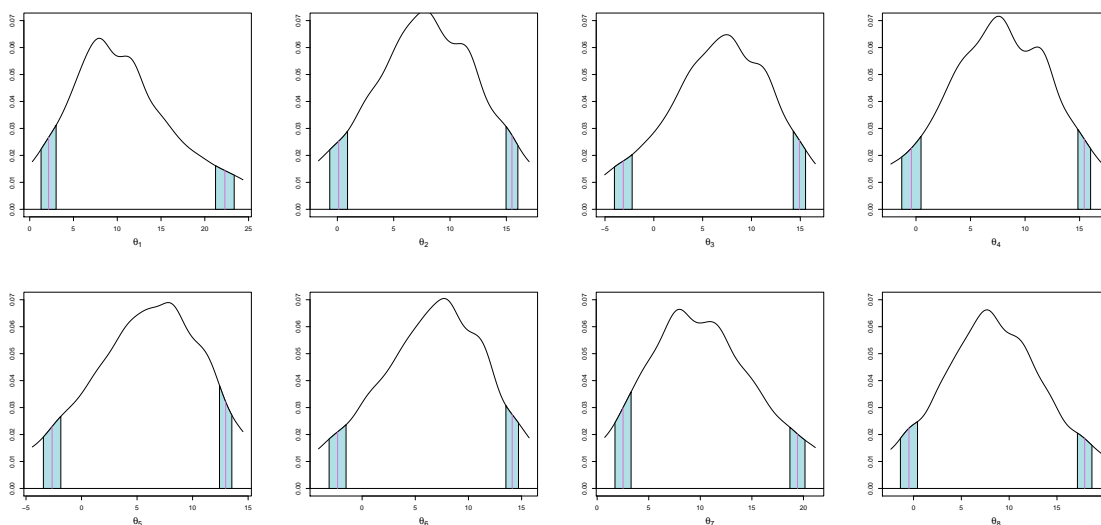


Figure 6: Plot of the estimates of an 80% credible interval for each θ with simultaneous 90% confidence intervals for 10,000 samples.

Consider, for $j = 1, \dots, J$, the hierarchical model

$$Y_j \mid \theta_j \sim N(\theta_j, \sigma_j^2)$$

$$\theta_j \sim N(\mu, \tau^2),$$

with σ_j^2 known and priors $f(\mu) \propto 1$ and $f(\tau) \propto 1/\tau$. The school data are comprised of estimated effects on student performance on verbal SAT scores after undergoing a coaching program. There are 8 schools in the sample for which each y_j is an estimated effect and σ_j is a known standard error for school j . We are interested in estimating features of the posterior distributions of the θ_j 's, the coaching effect for each school. To estimate this we simulate draws from the joint posterior $\theta, \mu, \tau \mid y$ with a deterministic scan Gibbs sampler

using the following full conditional distributions

$$\theta_j | \mu, \tau, y \sim N \left(\frac{y_j \tau^2 + \mu \sigma_j^2}{\tau^2 + \sigma_j^2}, \frac{1}{\frac{1}{\sigma_j^2} + \frac{1}{\tau^2}} \right), \quad \mu | \theta, \tau, y \sim N \left(\bar{\theta}, \frac{\tau^2}{J} \right), \quad \text{and}$$

$$\tau^2 | \theta, \mu, y \sim \text{Inv} - \chi^2 \left(J - 1, \frac{1}{J - 1} \sum_{j=1}^J (\theta_j - \mu)^2 \right),$$

where $\bar{\theta}$ is the average of the θ_j 's.

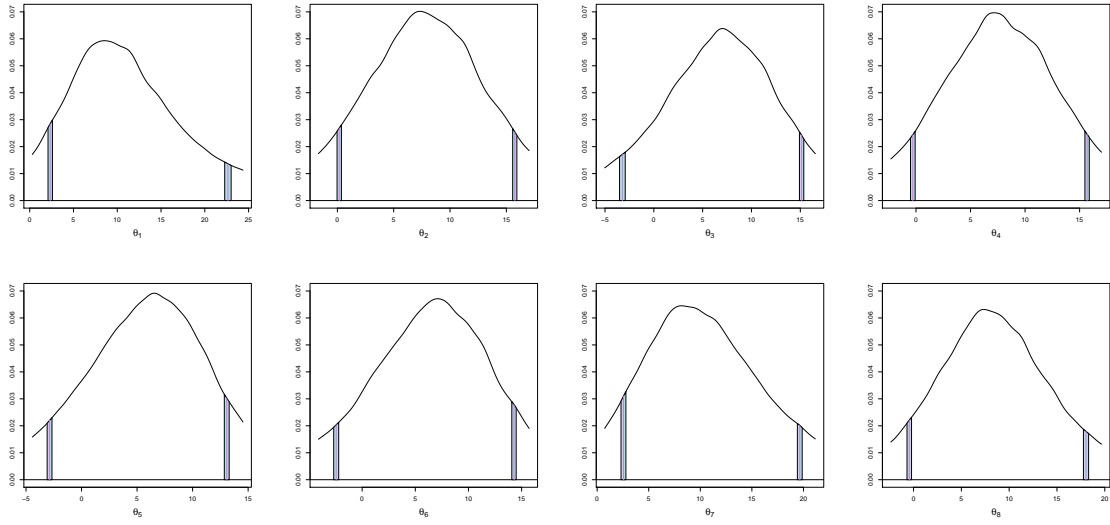


Figure 7: Plot of the estimates of an 80% credible interval for each θ with simultaneous 90% confidence intervals for 100,000 samples.

One might only be interested in credible intervals for each parameter. In Figure 6 we plot the simultaneous intervals in the form of marginal plots from 10,000 samples, while recalling that the simulation uncertainty estimates incorporate the full covariance structure. Many of the plots have similar shapes but different scales, thus some care should be taken in interpreting the length of each error region in each plot. Figure 7 presents the same analysis from a sample of 100,000, for which the simulation uncertainty of each quantity is substantially smaller. Figures 6 and 7 illustrate one reason accounting for simulation uncertainty can be important. Consider the left endpoints of the credible regions in the plots for θ_2 and θ_8 . Notice that in Figure 6 the left endpoints are indistinguishable from zero when we account for the Monte Carlo error, but this is no longer an issue with Figure 7.

Our procedure allows us to display something akin to the output of a **Stan** plot. Figure 8

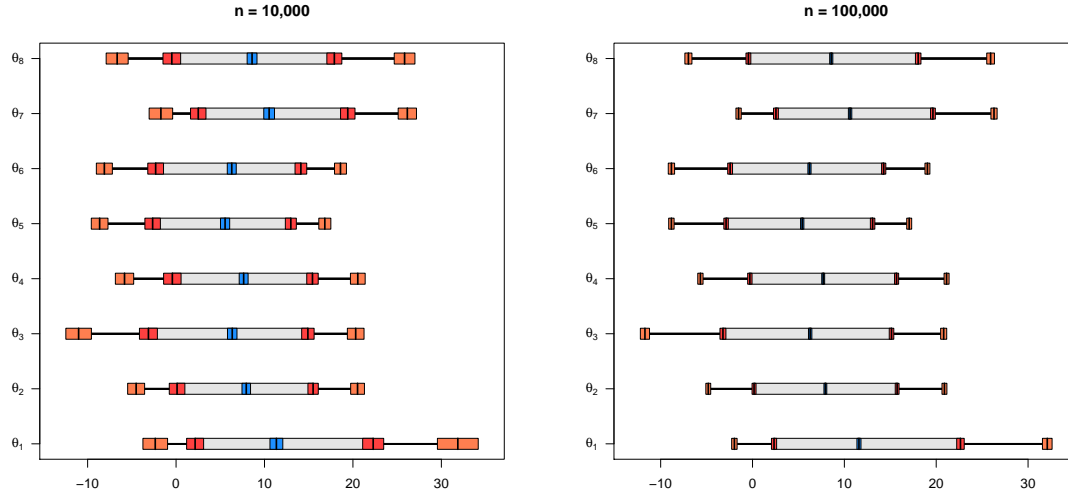


Figure 8: Boxplot inspired design where blue, red, and orange boxes correspond to a simultaneous 90% confidence level uncertainty of the posterior mean, 80% and 95% credible intervals, respectively.

includes a mean estimate and both an 80% and 95% credible interval for each θ in a boxplot inspired design. To make this plot, we estimated the resulting 40-dimensional $(\theta_g, \phi)'$ vector and covariance matrix. This approach makes it perhaps easier to compare the size of error regions around each estimate but discards the information gained by examining the marginal densities. Additionally, this sort of visualization requires each θ to be on a similar scale. Once again the sample size determines the size of the confidence regions, with $n = 100,000$ having substantially less simulation uncertainty.

5 Discussion

We provide a novel flexible class of visualizations for assessing the quality of estimation for Monte Carlo sampling. These visualizations are particularly helpful addressing concerns of Monte Carlo sample sizes and may be applied to a wide variety of problems including Monte Carlo estimation of expectations and quantiles, simulation studies, and visualization of a Bayesian analysis. The marginal-friendly interpretation retains more information than previously available methods. The line search algorithm that yields the $1 - \alpha$ simultaneous confidence intervals can be more widely applied to any statistic with an approximately multivariate normal sampling distribution (e.g. maximum likelihood estimators).

One issue not addressed is the case of a large number of quantities of interest, particularly

in MCMC sampling. In these cases, downward bias exhibited by batch means may lead to noticeable undercoverage of the simultaneous intervals. Other variance estimators such as weighted batch means or a lugsail window function (Vats and Flegal, 2018) may be used to induce upward bias to combat undercoverage. Additionally, our methods are only as good as the sampling method allows. A poor sampler may not provide representative samples from the target yielding misleading results or could require an enormous number of samples to be meaningful. We have offered no sampling guidance, but note this is a fundamental challenge in MCMC simulations (see e.g. Brooks et al., 2010; Fishman, 1996).

Acknowledgements

The authors thank Vladimir Minin for helping motivate our Bayesian analysis visualizations.

References

- Andrews, D. (1991). Heteroskedasticity and autocorrelation consistent covariant matrix estimation. *Econometrica*, 59:817–858.
- Babu, G. J. and Rao, C. R. (1988). Joint asymptotic distribution of marginal quantiles and quantile functions in samples from a multivariate population. *Journal of Multivariate Analysis*, 27:15–23.
- Bahadur, R. R. (1966). A note on quantiles in large samples. *The Annals of Mathematical Statistics*, 37:577–580.
- Blum, J. and Hanson, D. (1960). On the mean ergodic theorem for subsequences. *Bulletin of the American Mathematical Society*, 66:308–311.
- Bradley, R. C. (1986). Basic properties of strong mixing conditions. In Eberlein, E. and Taqqu, M. S., editors, *Dependence in Probability and Statistics: A Survey of Recent Results*, pages 165–192. Birkhauser, Cambridge, MA.
- Bradley, R. C. (2005). Basic properties of strong mixing conditions. a survey and some open questions. *Probability surveys*, 2:107–144.
- Brooks, S., Gelman, A., Jones, G., and Meng, X. (2010). *Handbook of Markov Chain Monte Carlo: Methods and Applications*. Chapman & Hall.
- Chan, K. W. and Yau, C. Y. (2017). Automatic optimal batch size selection for recursive estimators of time-average covariance matrix. *Journal of the American Statistical Association*, 112:1076–1089.
- Chen, D.-F. R. and Seila, A. F. (1987). Multivariate inference in stationary simulation using batch means. In *Proceedings of the 19th conference on Winter simulation*, pages 302–304. ACM.

- Dai, N. and Jones, G. L. (2017). Multivariate initial sequence estimators in Markov chain Monte Carlo. *Journal of Multivariate Analysis*, 159:184–199.
- Doss, C., Flegal, J. M., Jones, G. L., and Neath, R. C. (2014). Markov chain Monte Carlo estimation of quantiles. *Electronic Journal of Statistics*, 8:2448–2478.
- Ferguson, T. S. (1998). Asymptotic joint distribution of sample mean and a sample quantile. Technical report, UCLA.
- Fishman, G. S. (1996). *Monte Carlo: Concepts, Algorithms, and Applications*. Springer, New York.
- Flegal, J. M., Haran, M., and Jones, G. L. (2008). Markov chain Monte Carlo: Can we trust the third significant figure? *Statistical Science*, 23:250–260.
- Friedman, J., Hastie, T., and Tibshirani, R. (2009). glmnet: Lasso and elastic-net regularized generalized linear models. *R package version*, 1.
- Gelman, A., Carlin, J. B., Stern, H. S., and Rubin, D. B. (2004). *Bayesian Data Analysis*. Chapman & Hall/CRC, Boca Raton, second edition.
- Genz, A., Bretz, F., Miwa, T., Mi, X., Leisch, F., Scheipl, F., and Hothorn, T. (2018). mvtnorm: Multivariate Normal and t distributions. R package version 1.0-8.
- Ghosh, J. K. (1971). A new proof of the Bahadur representation of quantiles and an application. *The Annals of Mathematical Statistics*, pages 1957–1961.
- Hobert, J. P., Jones, G. L., Presnell, B., and Rosenthal, J. S. (2002). On the applicability of regenerative simulation in Markov chain Monte Carlo. *Biometrika*, 89:731–743.
- Hoerl, A. E. and Kennard, R. W. (1970). Ridge regression: Biased estimation for nonorthogonal problems. *Technometrics*, 12:55–67.
- Ibragimov, I. A. (1962). Some limit theorems for stationary processes. *Theory of Probability and Its Applications*, 7:349–382.
- Ibragimov, I. A. and Linnik, Y. V. (1971). *Independent and Stationary Sequences of Random Variables*. Walters-Noordhoff, The Netherlands.
- Jones, G. L. (2004). On the Markov chain central limit theorem. *Probability Surveys*, 1:299–320.
- Kay, M. (2018). tidybayes: Tidy data and geoms for Bayesian models. R package version 1.0.3.
- Koehler, E., Brown, E., and Haneuse, S. J.-P. A. (2009). On the assessment of Monte Carlo error in simulation-based statistical analyses. *The American Statistician*, 63:155–162.
- Lin, P.-E., Wu, K.-T., and Ahmad, I. A. (1980). Asymptotic joint distribution of sample quantiles and sample mean with applications. *Communications in Statistics-Theory and Methods*, 9:51–60.

- Liu, Y. and Flegal, J. M. (2018). Weighted batch means estimators in Markov chain Monte Carlo. *Electron. J. Statist.*, 12:3397–3442.
- Meyn, S. and Tweedie, R. (2009). *Markov Chains and Stochastic Stability*, volume 2. Cambridge University Press Cambridge.
- Priestley, M. B. (1981). *Spectral Analysis and Time Series. (Vol. 1): Univariate Series*. Academic Press.
- Seila, A. F. (1982). Multivariate estimation in regenerative simulation. *Operations Research Letters*, 1:153–156.
- Serfling, R. J. (1981). *Approximation Theorems of Mathematical Statistics (Wiley Series in Probability and Statistics)*. Wiley-Interscience.
- Shubin, M. (2015). Principles of posterior visualization [blog post]. Retrieved from <https://ctg2pi.wordpress.com/2015/02/24/principles-of-posterior-visualization>.
- Stan Development Team (2018). RStan: the R interface to Stan. R package version 2.17.4.
- Stigler, S. M. (1973). Studies in the History of Probability and Statistics. XXXII: Laplace, Fisher, and the discovery of the concept of sufficiency. *Biometrika*, 60:439–445.
- Tibshirani, R. (1996). Regression shrinkage and selection via the lasso. *Journal of the Royal Statistical Society: Series B*, 58:267–288.
- Vats, D. and Flegal, J. M. (2018). Lugsail lag windows and their application to MCMC. *ArXiv e-prints*.
- Vats, D., Flegal, J. M., and Jones, G. L. (2018). Strong consistency of multivariate spectral variance estimators in Markov chain Monte Carlo. *Bernoulli*, 24:1860–1909.
- Vats, D., Flegal, J. M., and Jones, G. L. (2019). Multivariate output analysis for Markov chain Monte Carlo. *Biometrika* (forthcoming).
- Wang, X., Hu, S., and Yang, W. (2011). The Bahadur representation for sample quantiles under strongly mixing sequence. *Journal of Statistical Planning and Inference*, 141:655–662.
- Yoshihara, K. (1995). The Bahadur representation of sample quantiles for sequences of strongly mixing random variables. *Statistics & Probability Letters*, 24:299–304.